Vol. 1, No. 1, pp. 7-12, December 2002

INTERNATIONAL JOURNAL OF SAFETY
www.kiis.or.kr

The Impact Stresses and Wave Propagation of Laminated Composites

Kook Chan Ahn*, Doo Hwan Kim[1] and Gwang Seok Lee[2]

**Department of Mechanical Design Engineering, Jinju National University, Jinju, 660-758, Korea*
[1]Department of International Livestock Industry, Jinju National University, Jinju, 660-758, Korea
[2]Department of Electronic Engineering, Jinju National University, Jinju, 660-758, Korea

(Received September 2, 2002; Accepted December 3, 2002)

Abstract : This paper demonstrates the impact stresses and wave propagation characteristics of glass/epoxy laminates subjected to the low-velocity impact by a steel ball theoretically and experimentally. A plate finite element model in conjunction with experimental contact laws is used for the theoretical investigation. The specimens for statical indentation and impact test are composed of $[0/45/0/-45/0]_{2s}$ and $[90/45/90/-45/90]_{2s}$ stacking sequences and have clamped-simply supported boundary conditions. Finally, these two results are compared and then the impulsive stress and wave propagation characteristics of this laminated composite are studied.

Key words : impact, impact stresses, finite element model, laminate composites, wave propagation

1. Introduction

Stress waves in composite materials are of interest to the engineers both for their constructive use and for the potential damage that can occur when short duration stress pulses propagate in a structure. The hard object impact usually gives a short contact time and results in the initial transmission of impact energy into a local region of the structure. This initial energy will propagate into the rest of the structure in the form of stress waves. Far field damage away from the impact agreed that the cause of the sudden failure must be examined from the point of transient wave propagation phenomena [1].

The impulsive stresses and wave propagation phenomena induced by impact loads in laminated composites are more complicated than those in homogeneous and isotropic plates due to the anisotropic and nonhomogeneous properties in the laminate.

A survey of wave propagation and impact in composite materials has been given by [2] many analytical [3, 4] and experimental [5~7] methods have been employed to study the wave propagation problems but many numerical [8, 9] methods have not been used for these investigations.

In this study, the impulsive stresses and wave propagation characteristics of glass/epoxy laminates due to the transverse low-velocity impact by a steel ball are investigated thoretically and experimentally. For theoretical analysis a dynamic finite element model in conjunction with static contact laws by experiment is used and impact experiment using surface strain gages on the laminated plate is carried and then the impulsive stress and wave propagation phenomena of this laminated composite are investigated.

*Corresponding author: kcahn@jinju.ac.kr

2. Theoretical Analysis

Consider a plate of uniform thickness h composed of a finite number of anisotropic layers with arbitary orientations. The coordinate system is chosen such that the middle plane, R, of the plate coincides with the x-y plane with z-axis normal to the middle plane.

The displacement field in the shear deformable theory is given by

$$\begin{aligned} u(x, y, z, t) &= u_0(x, y, t) - z\phi_x(x, y, t) \\ v(x, y, z, t) &= v_0(x, y, t) - z\phi(x, y, t) \\ w(x, y, z, t) &= w^0(x, y, t) \end{aligned} \quad (1)$$

Where u, v and w are the displacements along x, y and z directions respectively, u_0 and v_0 are the in-plane, displacements of the middle plane, ϕ_x and ϕ_y are the

shear rotations, and t is time.

The stress-strain relations of k-th lamina in laminate reference axes(x, y, t) is

$$\begin{Bmatrix}\sigma_{xx}\\ \sigma_{yy}\\ \sigma_{xy}\\ \sigma_{yz}\\ \sigma_{zx}\end{Bmatrix}^k = \begin{pmatrix}\overline{Q}_{11} & \overline{Q}_{12} & \overline{Q}_{16} & 0 & 0\\ \overline{Q}_{12} & \overline{Q}_{22} & \overline{Q}_{26} & 0 & 0\\ \overline{Q}_{16} & \overline{Q}_{26} & \overline{Q}_{66} & 0 & 0\\ & & & \overline{Q}_{44} & \overline{Q}_{45}\\ & & & \overline{Q}_{45} & \overline{Q}_{55}\end{pmatrix}^k \begin{Bmatrix}\varepsilon_{xx}\\ \varepsilon_{yy}\\ \gamma_{xy}\\ \gamma_{yz}\\ \gamma_{zx}\end{Bmatrix}^k \tag{2}$$

where

$$\{\varepsilon\}^k = \begin{Bmatrix}\varepsilon_{xx}\\ \varepsilon_{yy}\\ \gamma_{xy}\\ \gamma_{yz}\\ \gamma_{zx}\end{Bmatrix}^k = \begin{Bmatrix}\varepsilon^0\\ 0\end{Bmatrix} + \begin{Bmatrix}zx\\ \gamma_z^0\end{Bmatrix}$$

$$\{\varepsilon^0\} = \begin{Bmatrix}u^0_{,x}\\ v^0_{,y}\\ u^0_{,y} + v^0_{,x}\end{Bmatrix}$$

$$\{\chi\} = \begin{Bmatrix}-\phi_{x,x}\\ -\phi_{y,y}\\ -(\phi_{x,y} + \phi_{y,x})\end{Bmatrix}$$

$$\{\gamma_z^0\} = \begin{Bmatrix}\omega_{,y} & \phi_y\\ \omega_{,x} & \phi_x\end{Bmatrix} \tag{3}$$

in which σ_{ij} are stresses, ε_{ij} are strains and $\overline{Q}_{ij}$ are the material coefficients in the plate coordinates.

Assuming monoclinic behavior (i.e., existence of one plane of elastic symmetry) for each layer, the constitutive equations for an arbitrarily laminated plate are

$$\begin{Bmatrix}N\\ M\\ Q\end{Bmatrix} = \begin{Bmatrix}A & B & 0\\ B & D & 0\\ 0 & 0 & H\end{Bmatrix}\begin{Bmatrix}\varepsilon^0\\ \chi\\ \gamma_z^0\end{Bmatrix} \tag{4}$$

The plate stiffness A_{ij}, B_{ij}, D_{ij} and H_{ij} are given by

$$(A_{ij}, B_{ij}, D_{ij}) = \int_{-h/2}^{h/2} Q_{ij}(1, z, z^2)dz \ (i,j = 1, 2, 6)$$

$$H_{ij} = \int_{-h/2}^{h/2} \chi_i\chi_j\overline{Q}_{ij}dz \ (i,j = 4, 5) \tag{5}$$

where χ_i are the shear correction coefficients.

The equilibrium equations are given by

$$\begin{aligned}
N_{x,x} + N_{xy,y} &= P\ddot{u}^0 + R\ddot{\phi}_x\\
N_{xy,x} + N_{y,y} &= P\ddot{u}^0 + R\ddot{\phi}_x\\
M_{x,x} + M_{xy,y} - Q_x &= R\ddot{u}^0 + I\ddot{\phi}_x\\
M_{xy,x} + M_{y,y} - Q_y &= R\ddot{v}^0 + I\ddot{\phi}_y\\
Q_{x,x} + Q_{y,y} + q &= P\ddot{w}^0
\end{aligned} \tag{6}$$

where P, R and I are the normal, coupled nomal-rotary and rotary inertia coefficients,

$$(P, R, I) = \int_{-h/2}^{h/2} \rho^{(m)}(1, z, z^2)dz \tag{7.a}$$

$\rho^{(m)}$ being the material density of the m-th layer.

In Eq. (6), q is the transversely distributed force, and N_i, Q_i and M_i are the stress and moment resultants defined by

$$\begin{aligned}
(N_x, N_y, N_{xy}) &= \int_{-h/2}^{n/\angle} (\sigma_x, \sigma_y, \sigma_{xy})dz\\
(M_x, M_y, M_{xy}) &= \int_{-h/2}^{n/\angle} (\sigma_x, \sigma_y, \sigma_{xy})zdz\\
(Q_x, Q_y) &= \int_{-h/2}^{n/\angle} (\sigma_{zx}, \sigma_{yz})dz
\end{aligned} \tag{7.b}$$

Following the standard finite element procedure using above equations, we obtain the equations of motion the impactor-plate system

$$\begin{aligned}
F &= -m_s\ddot{w}_s = -ka^n \quad \text{(for loading process)}\\
&= F_m\left(\frac{\alpha - \alpha_0}{\alpha_m - \alpha_0}\right)^q \quad \text{(for unloading process)}
\end{aligned} \tag{8}$$

and

$$[M]\{\ddot{\Delta}\} + [K]\{\ddot{\Delta}\} = \{F\} \tag{9}$$

where m_s is the mass of impactor, k is the contact coefficient, F_m is the maximum contact force, α_m is the indentation in F_m, α_0 is the permanent indentation, $[M]$ is the mass matix, $[K]$ is the linear elastic stiffness matrix and $\{F\}$ is the contact force vector.

The contact force F between the plate and the impac-

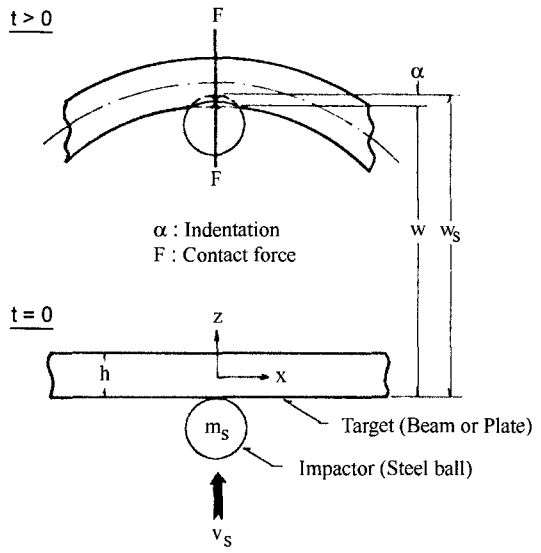

Fig. 1. Central transverse impact of a rigid body.

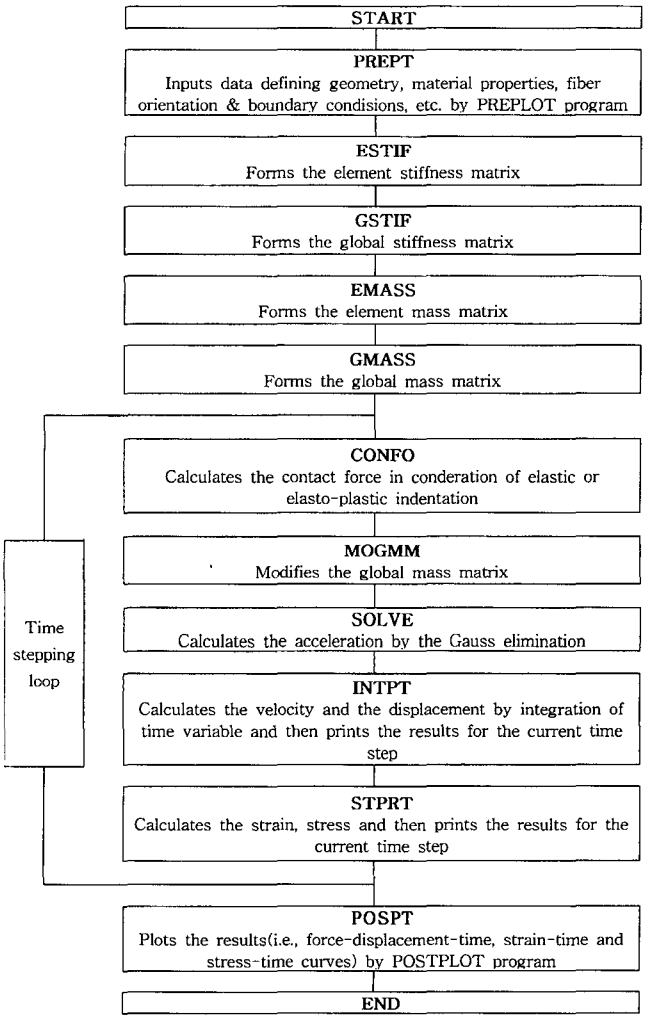

Fig. 2. Flow diagram for impact analysis of laminated composites.

tor is calculated by Eq. (8) and must be calculated before the Eq. (9) can be analyzed.

In this Eq. (8), indentation α is given by

$$\alpha = w_s(t+\Delta t) - w(x_0, y_0, t+\Delta t) \tag{10}$$

in which w and w_s is the plate and impactor deflection at the impact point (x_0, y_0), respectively (Fig. 1).

The finite element model used here is a four-node isoparametric quadrilateral element. Five degrees of freedom $\{\Delta\}_i = [u_i^0, v_i^0, w_i, \phi_{xi}, \phi_{yi}]^T$ are assumed at each node.

In the numerical integration of the stiffness $[K]$, the so-called reduced integration method is employed. The 2×2 Gaussian rule is used to compute the stiffness coefficients for the in-plane and bending deformation of the transverse shear deformation.

The solution for the equations for motion given by Eqs. (8)~(9) can be solved by time integration algorithm [10]. Flow diagram for impact analysis of laminated composites is shown in Fig. 2.

3. Experiment

3-1. Specimens

Stacking sequences of the specimens for static indentation and impact test were $[0/45/0/-45/0]_{2s}$ and $[90/45/90/-45/90]_{2s}$, and dimensions were $4.5^t \times 30^w \times 200^l$(mm) and $4.5^t \times 30^w \times 300^l$(mm).

In all tests, the specimens had clamped-simply supported boundary conditions. For material properties of the specimens, the tensile tests using specimens by ASTM rule were carried out. These results were shown in Table 1.

3-2. Static Indentation Test

The dial gage was mounted on a "⊂" bracket fixed to the loading piston so that only the relative displacement between the indentor and the specimens was recorded. The load was applied by Universal Test Machine (UTM25T) in loading and unloading processes and *x-y* plotter was used to obtain continuous force-indentation curves. A spherical indentor of diameter 12.7 mm was used.

These experimental static contact laws for loading and unloading processes are used for a dynamic finite element analysis.

3-3. Impact Test

The strain responses at two points on the plate were

Table 1. Material properties of the specimen and ball

	E_1	E_2	G_{12}	ν_{12}	r
Unit	N/mm2	N/mm2	N/mm2		N-sec^2/mm^4
Specimen	$5.585*10^4$	$1.475*10^4$	$0.643*10^4$	0.31	$0.205*10^{-8}$
Ball	$0.207*10^6$	$0.207*10^6$	$0.796*10^6$	0.30	$0.786*10^{-8}$

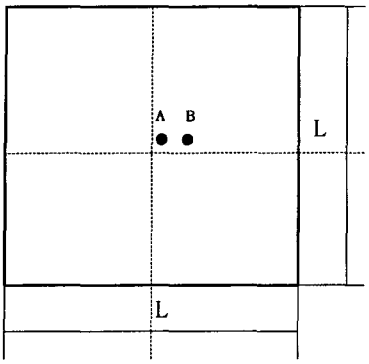

L : 200(300)mm
A : 2.1mm from impact point for 200mm
3.2mm from impact point for 300mm
B : 44.2mm from impact point for 200mm
66.3mm from impact point for 300mm

Fig. 3. Measuring points for strain response.

measured by means of surface strain gages. Two strain gages were placed at different locations as shown in Fig. 3 to record the dynamic strain histories. Impact velocity is 4 m/sec. and diameter of impactor is 12.7 mm. Signals from gages were amplified by a dynamic strain amplifier and recorded at the F.F.T.

4. Results and Discussion

The contact laws for the 12.7 mm steel indentor and glass/epoxy laminate were determined experimentally by means of a statical indentation test. The plate specimens were fitted into power equations by least square method and their results were shown in Fig. 4.

The statically determined contact laws were incorporated into an developed four-node isoparametric plate finite element program to obtain the impact response of glass/epoxy laminated plate due to impact.

An impact experiment was conducted on a glass/epoxy laminates plate to verify the validity of the dynamic finite element analysis. The overall trends of strain responses predicted using the finite element method agreed very well with the test results as shown in Figs. 5-8.

Through these theoretical and experimental strain

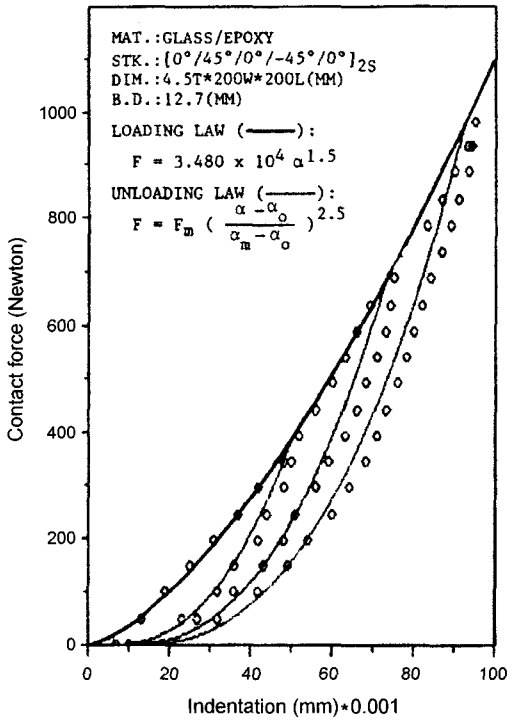

Fig. 4. Loading and unloading curves for $[0/45/0/-45/0]_{2s}$ glass/epoxy laminate.

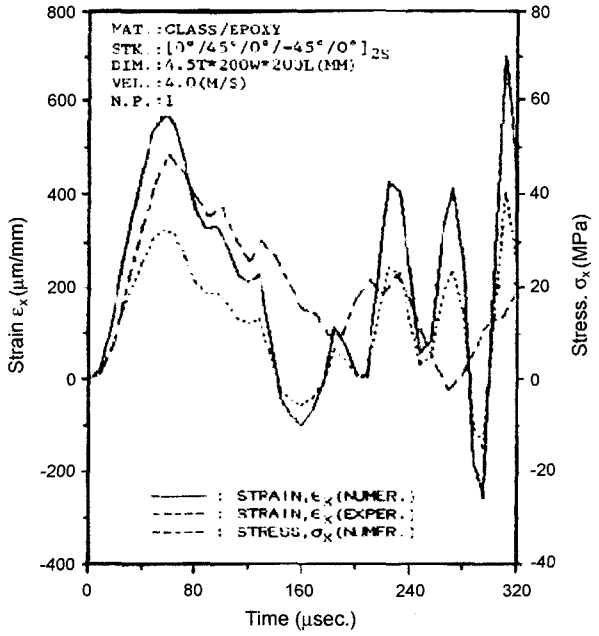

Fig. 5. Strain and stress response histories for a $[0/45/0/-45/0]_{2s}$ glass/epoxy laminate at 2.1 mm from the impact point.

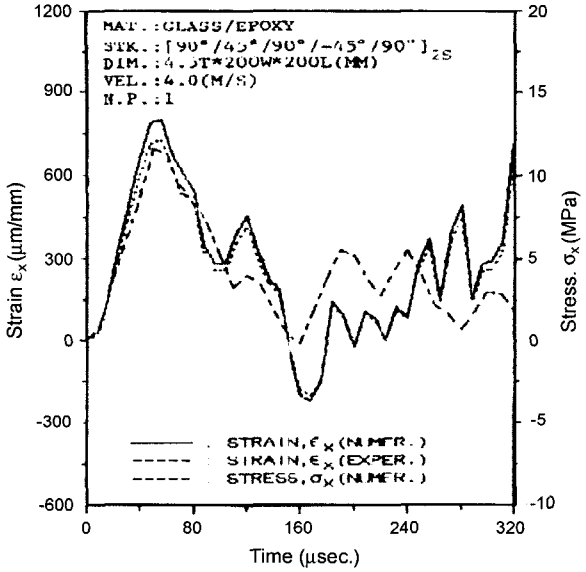

Fig. 6. Strain and stress response histories for a $[90/45/90/-45/90]_{2s}$ glass/epoxy laminate at 2.1 mm from the impact point.

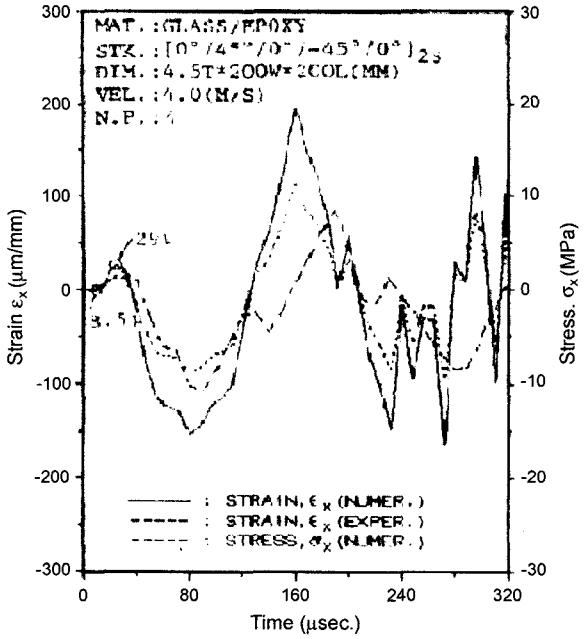

Fig. 7. Strain and stress response histories for a $[0/45/0/-45/0]_{2s}$ glass/epoxy laminate at 44.2 mm from the impact point.

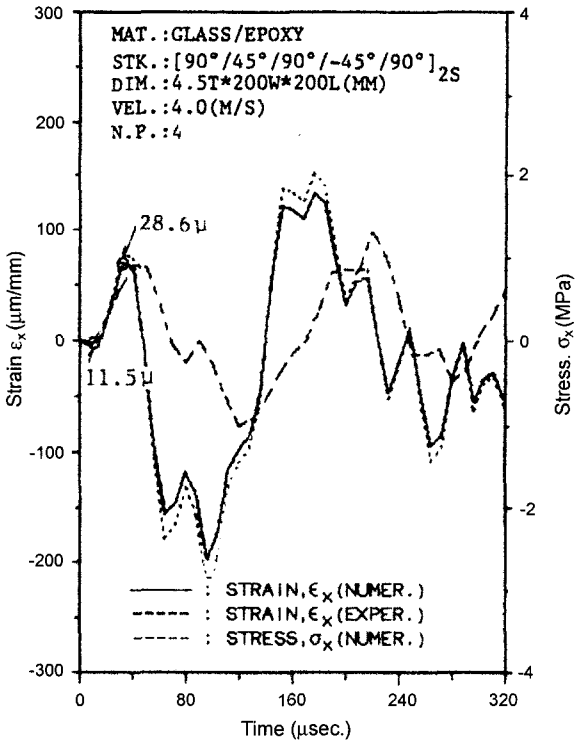

Fig. 8. Strain and stress response histories for a $[90/45/90/-45/90]_{2s}$ glass/epoxy laminate at 44.2 mm from the impact point.

(stress) responses, we could predict the impulsive strain (stress) in glass/epoxy laminated composite as shown in Table 2 and wave propagation characteristics in Table 3. That is, we could know appreciable modulus and strength degradation may be produced due to large strain (stress) in the neighborhood of the impact point and in special, large strain in the transverse to the fiber direction from Table 2. As shown in Table 3, the predominent wave induced by central impact has found to be a flexural one propagating at different velocities in different directions, and also the flexural wave velocity is higher in the higher modulus direction and the amplitude of the flexural wave is much larger than that of the in-plane wave.

Table 2. Comparison of maximum strain and maximum stress

Stacking sequence	Size	at 2.1 mm or 3.2 mm				at 44.2 mm or 66.3 mm	
		ε_x	σ_x	ε_y	σ_y	ε_x	σ_x
[0/45/0/-45/0]2s	200 mm	567	32.5	804	14.8	−155	−8.9
	300 mm	402	23.1	539	10.0	−87	−3.0
[90/45/90/-45/90]2s	200 mm	800	12.1	570	36.4	−198	−3.0
	300 mm	543	8.2	402	25.6	−112	−1.7

Table 3. Comparison of wave velocities (unit: m/sec)

Stacking sequence	$[0/45/0/-45/0]_{2s}$				$[90/45/90/-45/90]_{2s}$			
Specimen size(mm)	200	300	200	300	200	300	200	300
Wave type	C_L^0	C_L^0	C_L^0	C_F^{90}	C_L^0	C_L^0	C_F^{90}	C_F^{90}
Wave propagation theory	5,286		1,771		2,716		1,771	
Present simulation	5,200	4,736	1,668	1,432	3,844	3,400	1,270	1,367
Impact experiment	4,911	4,420	1,498	1,313	3,536	3,234	1,163	1,251

{Superscripts} 0: top part of [0/45/0/-45/0]2s laminate.
90: top part of [0/45/0/-45/0]2s laminate.
{Subscripts} L: longitudinal(in-plane) wave.
F: flexural(transverse) wave.

5. Conclusions

Through the theoretical and experimental impact responses, we obtain the following conclusions.

1) In general, theoretical in-plane and leading flexural wave velocities agreed well with the corresponding values by experiment.

2) The predominent wave induced by central impact has found to be a flexural one propagating at different velocities in different directions.

3) The flexural wave velocity is higher in the higher modulus direction and the amplitude of the flexural wave is much larger than that of the in-plane wave.

4) Appreciable modulus and strength degradation may be produced due to large strain(stress) in the neighborhood of the impact point and in special, large strain in the transverse to the fiber direction.

Acknowledgement

This work was supported by the Korea Science and Engineering Foundation (KOSEF) through the Regional Animal Industry Research Center.(Project No. : R12-2002-053-02003-0)

References

[1] W. Goldsmith, Impact, Edward Arnold Ltd., London, 1960.

[2] F.C. Moon, "A Critical Survey of Wave Propagation and Impact in Composite Materials", NASA CR-121226, 1973.

[3] C.T. Sun and S. Chattopadhyay, "Dynamic Response of Anisotropic Laminated Plates under Initial Stress to Impact of a Mass", Journal of Applied Mechanics, Trans. ASME, pp. 693-698, 1975.

[4] C.T. Sun and S.N. Huang, "Transverse Impact Problems by Higher Order Beam Finite Element", Computers & Structures, Vol. 5, pp. 297-303, 1975.

[5] I.M. Daniel, T. Liber and R.H.L aBedz, "Wave Propagation in Transversely Impacted Composite Laminates" Experimental Mechanics, pp. 9-16, 1979.

[6] T. Hayashi, R. Ugo and Y. Morimoto, "Experimental Observation of Stress Waves Propagating in Laminated Composites", Experimental Mechanics, pp. 169-174, 1986.

[7] N. Taketa, R.L. Sierakowski, L.E. Malvern, "Wave Propagation Experiments on Ballistically Im-pacted Composite Laminates", Journal of Composite Materials, Vol. 15, pp. 157-174, 1981.

[8] K.C. Ahn, M.S. Kim and G.N. Kim, "Impact Analysis of Laminate Composite Beams by the Finite Element Method", Transaction of KSME, Vol. 12, No. 4, pp. 652-661, 1988.

[9] K.C. Ahn, M.S. Kim and G.N. Kim, "A Study on the Impact Behaviour of the Beam-Like Laminate Composites by Beam and Plate Theory", Transaction of KSME, Vol. 13, No. 1, pp. 1031-1036, 1989.

[10] E.L. Wilson and R.W. Clough, "Dynamic Response by Step by Step Matrix Analysis", Symp. on Use of Computers in Civil Engineering, 1962.